MODELING OF THE COMBUSTION OSCILLATIONS AND SOOT FORMATION IN AEROVALVED PULSE COMBUSTORS

M. Moghiman and B. Rezapoor

Department of Mechanical Engineering, Ferdowsi University of Mashhad
Mashhad, Iran, mmoghiman@yahoo.com

(Received: July 1, 2002 – Accepted in Revised Form: May 15, 2003)

Abstract This paper describes the modifications and evolution of a thermal pulse combustion model for predicting the combustion oscillations of an aerovalved 250 kW pulse combustor incorporating a soot formation-combustion model. Validation of the model is carried out from the experimental data of an aerovalved Helmholtz type pulse combustor, where a sinusoidal air inlet mass flow coupled with pressure oscillations within the combustor is needed to model the instabilities of combustion oscillations correctly. The model is used to investigate the influence of different boundary conditions on combustion oscillations and soot production in the pulse combustor. The results identify the operating conditions for which continuous oscillations, steady flames and flame extinction occur. The results also show that for ambient temperatures of inlet air (lower than 325 K) with wall temperatures lower than 1100 K soot emission from propane firing pulse combustors is negligible.

Key Words Pulse Combustion, Aerovalved Pulse Combustor, Soot Formation

چکیده این مقاله توسعه و تکمیل یک مدل تحلیلی برای پیشگویی نواسانات احتراقی و تولید دوده را در یک محفظه احتراق ضربه ای با شیر هوایی و ظرفیت ۲۵۰ کیلو وات ارائه می‌کند. مقایسه نتایج مدل با داده های آزمایشگاهی نشان می‌دهد که برای پیشگویی صحیح ناپایداری های نوسانات احتراقی نیاز به جریان ورودی سینوسی هوا با در نظر گرفتن اثر نواسانات فشار در داخل محفظه احتراق می‌باشد. با استفاده از مدل اثر شرایط مرزی بر نوسانات احتراق و تولید دوده در داخل محفظه احتراق ضربه ای مورد مطالعه قرار گرفته و شرایط مورد نیاز برای تداوم نوسانات پایدار و همچنین شرایطی که شعله های بدون نوسان یا خاموشی شعله رخ می‌دهد، مورد تجزیه و تحلیل قرار گرفته است. نتایج نشان می‌دهد که برای هوای ورودی با دمای محیط و همچنین دمای دیواره کمتر از ۱۱۰۰ K تولید دوده در محفظه های احتراق ضربه ای با سوخت پروپان ناچیز است.

1. INTRODUCTION

The need for highly efficient combustion systems especially after the oil crisis of early seventies, has led to active research in pulse combustion. Pulsating combustion is a non-steady process that involves the coupling of a complicated transient flow field, generated by a transient energy release, with a resonant acoustic wave. Pulsed combustors have many advantages over conventional burners, such as high combustion and thermal efficiencies with low excess air values, high rates of heat transfer, high combustion intensities (the energy release per unit volume), self-aspiration, capability to burn a variety of fuels (including low quality fuels), and low emissions of NO_x and CO [1,2,3].

The pulse combustors are simple devices consisting principally of fuel and air inlet valves, a combustor chamber, and a resonance tube (tailpipe) for exhausting the combustion products (Figure 1). After the initial start-up the pulsating combustion process occurs spontaneously without the need of a spark plug. Periodic (pulse) combustion in the combustion chamber is driven /maintained by the acoustic mode in the tailpipe. The operation of the pulse combustor occurs in three phases [4]. In the first phase, ignition of the combustible mixture occurs by the remaining hot burned gas from the previous cycle. The burned gas expands and moves outwards the inlet and the exit of the combustion chamber. In the second phase the burned gas moves out through the tail pipe and the pressure in the combustion chamber falls. The pressure eventually falls below the atmospheric pressure (or upstream pressure) due to the momentum effect of the outward moving gases

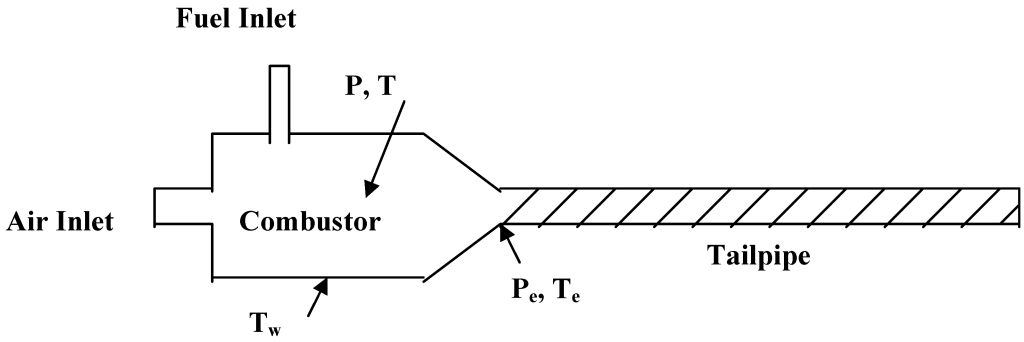

Figure 1. Sketch of pulse combustor consisting of fuel and air inlets, a combustion chamber and a tailpipe. The combustion chamber and tailpipe are joined by a transition section [8].

and the outflow slows down. In the third phase fuel and air enter the combustor. The momentum effects cause the pressure to rise above the ambient value. Due to high temperature in the combustor the mixture of fuel and air self-ignites and thus, the entire oscillating cycle repeats itself. Although there are several different types of pulse combustors (for example, the quarter wave or Schmidt tube, the Rijke tube, the Helmholtz resonator, and the Reynst pulse pot), the underlying principle controlling their operation is the same-namely; the periodic addition of heat must be in phase with the resonant pressure oscillations. This commonly referred to as Rayleigh's criterion. Pulse combustion technology has been utilized in a wide range [1,5]. The most useful application to date has been in the field of fluid heating. The gas burning Helmholtz type pulse combustors in particular have proven most popular in this area. Lennox, Hydrotherm, and Fulton and Pulsonex companies have achieved noted commercial success. In 1993 Lennox has sold over one million of warm air furnaces (12 to 38 kW) in the U.S. [5].

Studies have shown that the flow oscillations increase the rate of mass, momentum (i.e. mixing) and heat transfer [6,7]. Convective heat transfer rates from the oscillating flows, such as those found in a pulse combustor tailpipe, can be much higher than those of steady turbulent flows with the same mean Reynolds number [8,9]. The compactness of pulse combustors due to high heat transfer rates and the ability of these devices to pump their own air, completely independent of external energy sources, have intrigued designers of combustion equipment and have led to production low cost compact heat exchangers. Although pulse combustion can provide the inherent advantages described above, there are naturally restrictions and limitations of this technology. The limitations of pulse combustion technology are: excessive noise outputs, the destructive nature of the flow oscillations and sensitivity to gas composition. The sound pressure levels inherent to the pulse combustion process are often cited as a serious restriction. The noise emission can however be ameliorated through the use of appropriate silencing techniques including the decoupling chamber [10]. The periodic pressure oscillations and associated flow field inside a typical pulse combustor is inherently destructive. Pulse combustion devices need therefore to be constructed from suitable materials and be suitably mounted and located. Pulse combustors can also cause strong mechanical vibrations in nearby structures and machine components.

Two types of pulse combustor inlet valves have been developed: the aerodynamical-valve type and the mechanical-valve type [1]. In the aerovalve type combustors the cold air in the inlet confinement acts as a resistance for the gases in the combustion chamber to leave through the inlet. However, in practice a considerable amount of gas may flow through the inlet at the pressure part of the cycle. The mechanical valve inlet, such as a flopper valve, permits flow in only one direction.

Although the technology of pulse combustion has been known for many years, fundamental understanding of pulse combustion is limited

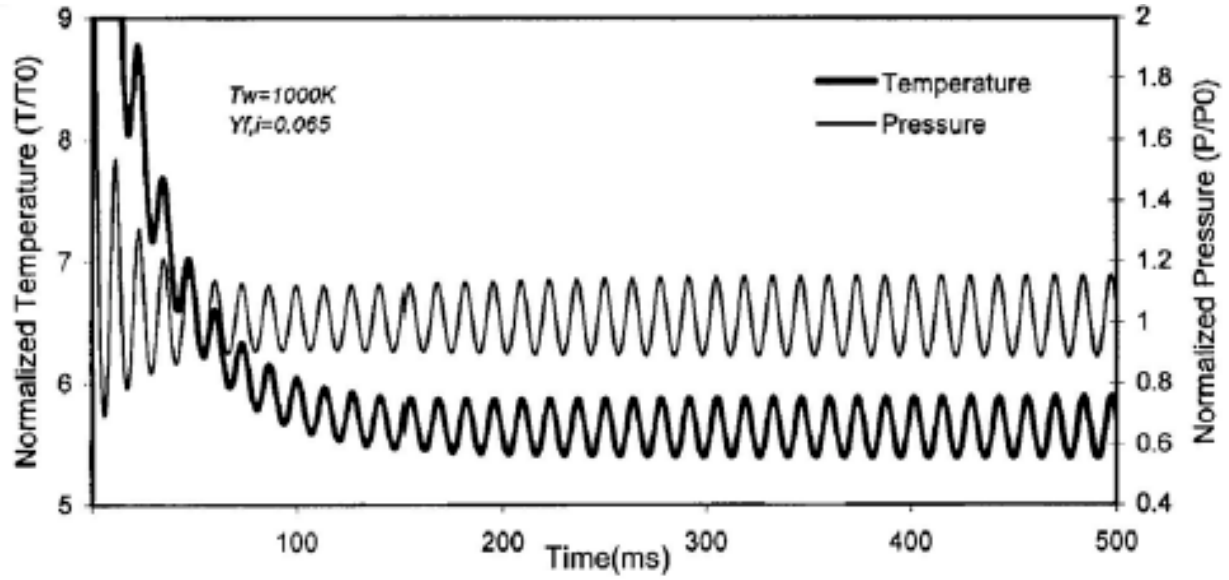

Figure 2. Predicted temperature and pressure history (0-500 ms) in the pulse combustor.

compared to that of rival combustion technologies [11,12]. Because of the lack of fundamental information the design and development of pulse combustors has proceeded largely by trail and error, a method that is time-consuming, costly, and that does not guarantee an optimum design. As the operating principle of pulse combustors based upon the coupling of a transient flow field with an acoustic pressure field, the simulation of the coupling of these flows is complicated. A number of theoretical models have been developed for simulation of pulse combustion [13-16]. Richard et al. [13] demonstrated theoretically and experimentally that relatively large amplitude combustion oscillations could be produced in a premixed pulse combustor. Tsujimoto and Machii [14] employed the method of characteristics in the modeling of a Helmholtz pulse combustor. They concluded that the periodic combustion delay time plays a significant role in the burner operation and that the processes that control this delay time are also important. Morel [15] gained results from a finite difference model that solves one-dimensional wave equations of mass, momentum and energy. Benelli et al. [16] presented preliminary results of 2D simulations of the Lennox Warm Air Furnace using the FLUENT software. Frequencies were accurately predicted, but timing of combustion to the correct phase, to satisfy Rayleigh Criterion, was problematic.

The purpose of this work is to develop and implement a phenomenological model of pulsating combustion for predicting the dominant feature of the process in an aerovalved pulse combustor for which experimental results are available. The model will be used to investigate the influence of valve dynamics, inlet fuel input and thermal boundary conditions on combustion oscillations and soot production in the pulse combustor.

Governing Equations The zero-dimensional model initially proposed by Richards et. al. [13] is used in this analysis. As this model considers stoichiometric condition with a steady supply of fuel and air mixture, the paper concentrates on modifications to incorporate the stoichiometric and non-stoichiometric of non-premixed supply (with the assumption that mixing occurs well ahead of the flame zone) and to account for soot production in the pulse combustor. The model geometry of pulse combustor is shown in ure 1.

Air Inlet Combustor Although fuel and air enter separately through two mass flow inlets, due to high mixing rates in the pulse combustors [1,4],

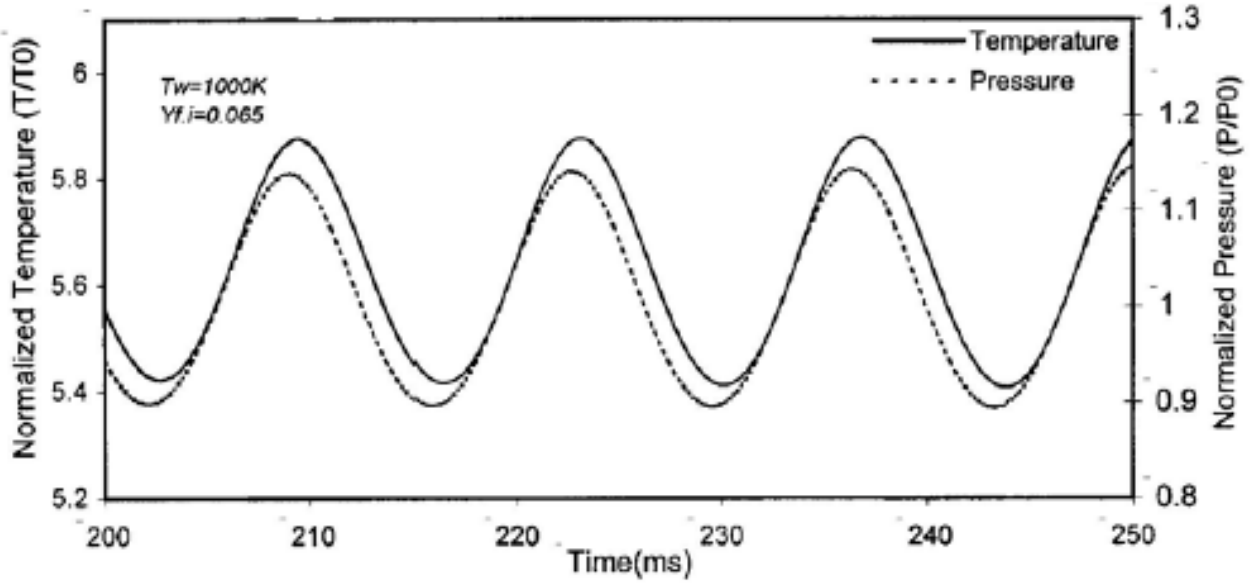

Figure 3. The frequency of oscillations in the pulse combustor.

the combustion zone control volume is treated as a well mixed region and the burning process is considered in terms of homogeneous premixed conditions [17]. The basic equations describing the combustion/acoustic oscillations are conservation equations for energy, mass and species in combustion chamber and momentum in the tailpipe. The control volume equation for energy conservation in the combustion zone is [13]:

$$\frac{d}{dt}\int_{cv}\rho\,\varepsilon\,dv+\oint_{cs}\rho\,\vec{v}.\hat{n}\varepsilon\,ds + \oint_{cs}p\vec{v}.\vec{n}ds+\oint_{cs}\vec{q}.\hat{n}ds=\int_{cv}Qdv \quad (1)$$

where $\varepsilon = e + (1/2)v^2$, e is specific internal energy, $(1/2)v^2$ is the specific kinetic energy, Q represents the heat release per unit volume from combustion and the vector $\vec{q}$ stands for heat transfer at the control volume interface. Thus, the term $\oint_{cs}\vec{q}.\hat{n}ds$ represents the control volume gain in thermal energy via heat transfer from the combustor wall. Equation 1 is simplified subjected to the following assumptions. The specific kinetic energy contributions, $v^2/2$, to the combustor volume are small compared to the specific internal energy, e. The combustor volume is considered as a homogeneous zone, and ideal gas property relations (including constant specific heat C_v) are used: $e = C_v T$, $\rho = P/RT$, $C_p = C_v + R$ and speed of sound is $\sqrt{\gamma RT}$. The surface integral is evaluated by specifying the instantaneous mass inlet and exit rates m_i and m_e. In the initial analysis, the inlet mass flow rates assumed to be constant throughout the cycle.

Using the above definitions and assumptions, and expressing the heat transfer in terms of the wall temperature T_w and heat transfer coefficient h, Equation 1 becomes:

$$\frac{1}{\gamma-1}\frac{dp}{dt}=C_p\left[\frac{m_iT_i}{V}-\frac{m_eT}{V}\right]+Q+\frac{hA_s}{V}\left(T_w-T\right) \quad (2)$$

where V is the combustion zone volume, A_s is the combustor surface area, γ is the specific-heat ratio, T_i is the inlet temperature and T_e is the combustor exit temperature.

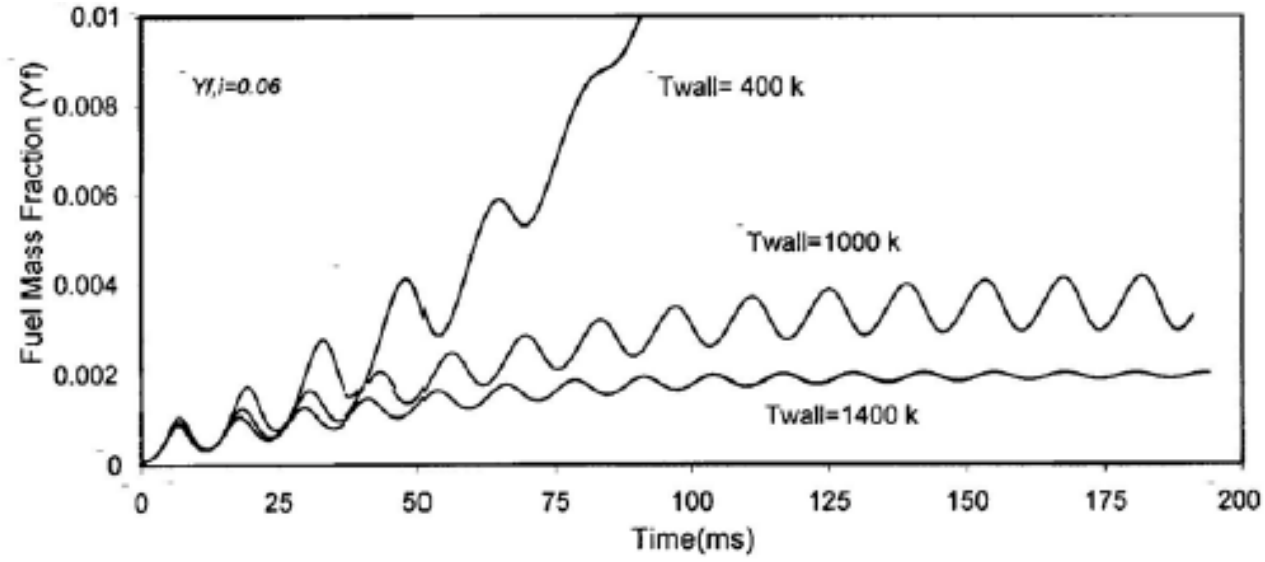

Figure 4. Effect of wall temperature on the fuel mass fraction oscillations.

From the balance equation for mass in the combustion zone, and using the above assumptions and simplifications:

$$\frac{d\rho}{dt} = \frac{m_i - m_e}{V} \tag{3}$$

which using $\rho = p/RT$ becomes:

$$\frac{1}{RT}\frac{dp}{dt} - \frac{p}{R}\frac{1}{T^2}\frac{dT}{dt} = \frac{m_i - m_e}{V} \tag{4}$$

Combining Equation 2 with Equation 4 and defining the following definitions and variables:

$z_i = m_i / V$
(Inlet mass flow per combustion zone volume) (5)

$z_e = me / V$
(Exit mass flow per combustion zone volume) (6)

$Lc_i = V/A_s$
(The first characteristic length) (7)

$\tau_f = \rho_o / zi$
(A characteristic flow time) (8)

$\tau_{HT} = (L_{c1}\rho_o C_p T_o) / (hT_w)$
(A characteristic heat transfer time) (9)

$\tau_c = (\rho_o C_p T_o) / Q$
(A characteristic combustion time) (10)

where subscript o denotes the ambient condition, and after normalizing pressure and temperature with ambient conditions, Equations 2 and 4 give:

$$\frac{d\tilde{T}}{dt} = \gamma\left\{\frac{1}{\tau_f} + \frac{1}{\tau_{HT}} + \frac{1}{\tau_c}\right\}\frac{\tilde{T}}{\tilde{p}} - \left\{(\gamma - 1)\frac{z_e}{\rho_o} + \frac{1}{\tau_f} + \frac{\gamma}{\tau_{HT}}\frac{T_o}{T_w}\right\}\frac{\tilde{T}^2}{\tilde{p}} \tag{11}$$

$$\frac{d\tilde{p}}{dt} = \gamma\left\{\frac{1}{\tau_f} + \frac{1}{\tau_{HT}} + \frac{1}{\tau_c}\right\} - \left\{\frac{z_e}{\rho_o} + \frac{\gamma}{\tau_{HT}}\frac{T_o}{T_w}\right\}\gamma\tilde{T} \tag{12}$$

where the tiled denotes the normalized temperature ($\tilde{T} = T/T_o$) and pressure ($\tilde{p} = p/P_o$). The

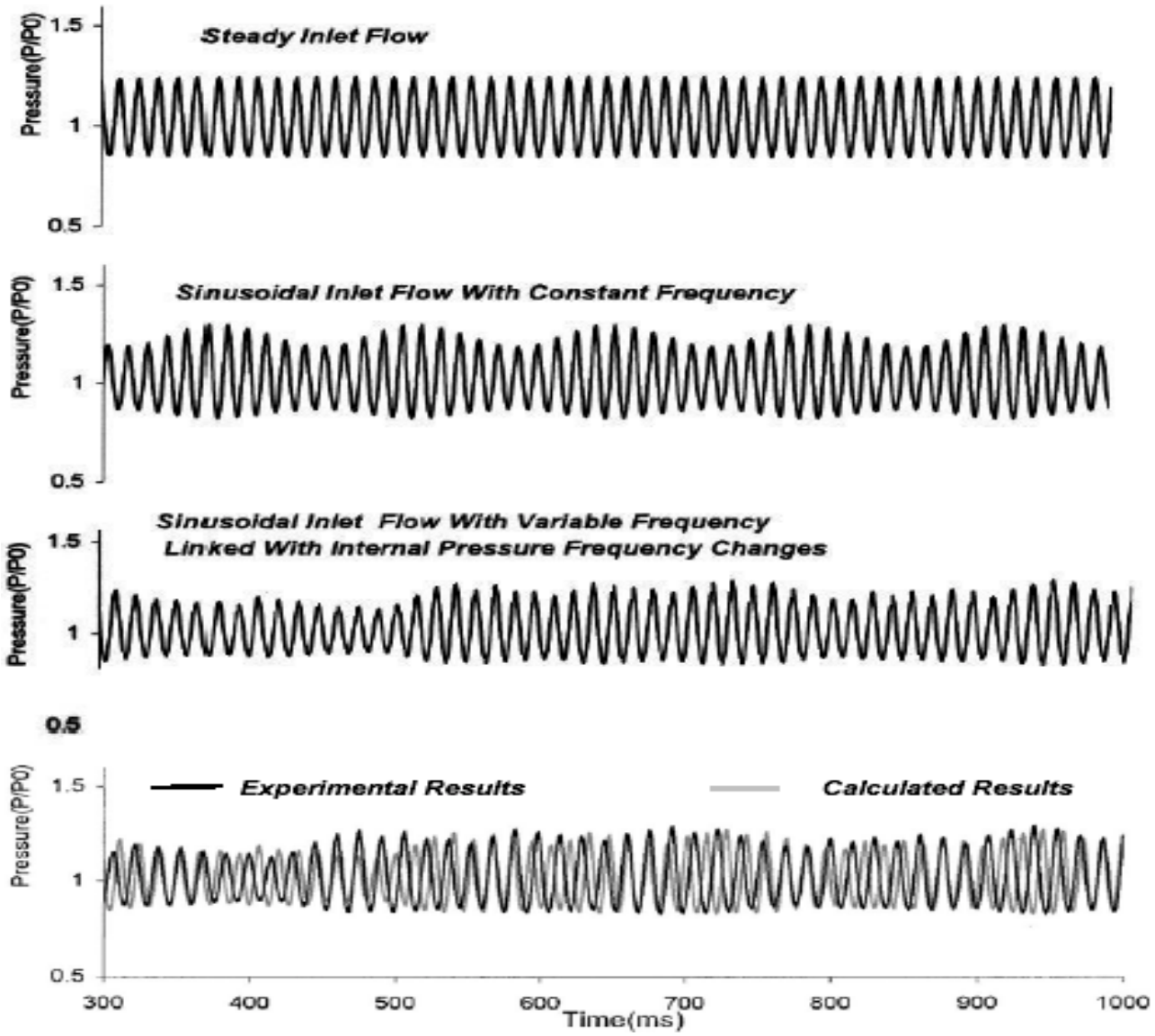

Figure 5. Comparison of calculated pressure oscillations with experimental results.

combustor exit temperature, T_e, and exit pressure, p_e, at the tailpipe entrance are related to p, T in the combustion chamber by the following isentropic acceleration (deceleration) relations from (into) the combustion chamber:

$$T_e = \tilde{T} + \frac{(1-\gamma)u^2}{2\gamma RT_o} \tag{13}$$

$$\tilde{p}_e = \tilde{p}\left(\frac{2\gamma RT_o\tilde{T}}{2\gamma RT_o\tilde{T} + (1-\gamma)u^2}\right)^{\frac{\gamma}{1-\gamma}} \tag{14}$$

where u is the velocity of the gas in the tailpipe, which is obtained from Equation 25.

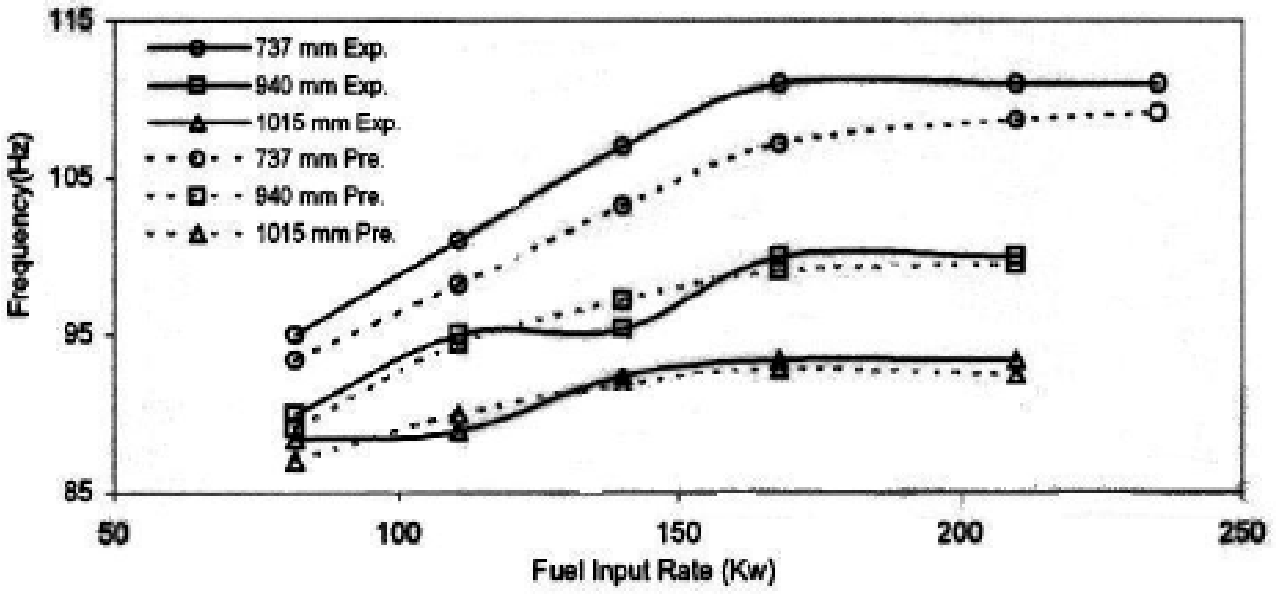

Figure 6. Comparison of calculated fundamental operating frequencies with experimental values.

Combustion Sub-Model To solve Equations 11 and 12 an expression for the instantaneous heat release per unit volume, Q, is needed. Q is the product of the heat of reaction, ΔH_f, and the fuel reaction rate, R_f :

$$Q = \Delta H_f . R_f \tag{15}$$

The value of ΔH_f for propane, the fuel used in the combustor considered in this study, is available in literature. Employing a one-step reaction combustion model between fuel (subscript f) and oxygen (subscript ox) the fuel reaction rate is given by [17]:

$$R_f = A T^{1/2} \rho^2 Y_{ox} Y_f e^{-E/RT} \tag{16}$$

where A is a kinetic constant, E is the activation energy, and Y_{ox}, Y_f are the instantaneous mass fractions of fuel and oxygen in the combustion chamber. The mass fractions are determined from a formulation of species balance in the combustor volume:

$$\frac{d}{dt}\int_{cv} \rho Y_f \, dV = -\oint \rho Y_f \vec{v}.\hat{n} ds - \int_{cv} R_f \, dV \tag{17}$$

This equation is simplified with the same assumptions used to derive Equation 2 from Equation 1. Performing the indicated integrations, under stoichiometric conditions, the resulting equation for fuel mass fraction is:

$$\frac{dY_f}{dt} = \left(Y_{f,i} - Y_f\right)\frac{\tilde{T}}{\tilde{p}}\frac{1}{\tau_f} - \frac{\tilde{T}}{\tilde{p}}\left(\frac{C_p T_o}{\Delta H_f}\right)\frac{1}{\tau_c} \tag{18}$$

where $Y_{f,i}$ is the inlet fuel mass fraction. Under stoichiometric conditions Y_{ox} can be substituted with $S_r Y_f$ (S_r is the stoichiometric mass ratio) in Equation 16 and so the fuel mass fraction can be calculated via Equation 18 alone, thus simplifying

the analysis. Under non-stoichiometric conditions the instantaneous oxygen mass fraction is not proportional to the instantaneous fuel mass fraction, and to obtain Y_{ox} an equation similar to Equation 18 for Y_{ox} can be derived:

$$\frac{dY_{ox}}{dt} = \left(Y_{ox,i} - Y_{ox}\right)\frac{\tilde{T}}{\tilde{p}}\frac{1}{\tau_f} - Y_{ox}\frac{\tilde{T}}{\tilde{p}}\frac{z_e}{\rho_o} - m_{ox,e}\frac{\tilde{T}}{\tilde{p}}\frac{1}{\rho_o V} - S_r\frac{\tilde{T}}{\tilde{p}}\left(\frac{C_p T_o}{\Delta H_f}\right)\frac{1}{\tau_c} \quad (19)$$

where $Y_{ox,i}$ is the instantaneous inlet oxygen mass fraction, $m_{ox,e}$ is the oxygen exit mass flow and S_r = 3.64.

From Equations 15, 16, and 10 the expression for the combustion time including the oxygen mass fraction is:

$$\frac{1}{\tau_c} = A'\frac{\Delta H_f}{C_p T_o}\frac{\tilde{p}^2}{\tilde{T}^{3/2}}Y_f\frac{Y_{ox}}{S_r}\exp\left(-E/RT\right) \quad (20)$$

where constant A' is the product of kinetic constant from Equation (16) multiplied by various other model constants ($A' = (A.P_o.S_r)/T_o^{1/2}$). Value for this kinetic constant is [6]: $A' = 3.85\times10^8$ s^{-1}.

Soot Formation Sub-Model An empirical soot model is used for the prediction of soot production in the pulse combustor. In this model the rate of soot formation is given by the following equation [18]:

$$\frac{dS}{dt} = C_S.T^{\alpha}.c_f^{\beta}.c_{ox}^{\theta}.\exp(-E/RT) \qquad \left(\frac{g}{cm^3.s}\right) \quad (21)$$

where c_f and c_{ox} stand for fuel and oxygen concentrations, respectively, and the values of rate constants are as follow:

$C_S = 4.66\times10^{14}$, $\alpha = -1.94$, $\beta = 1.81$, $\theta = -0.5$

The soot combustion is modeled by the post-flame oxidation expression introduced by Nagle and Strickland-constable [19], which has been widely used by several investigators [18,20]. The rate of soot combustion per unit area of soot surface is as follows:

$$\frac{dS_c}{dt} = \left(\frac{k_A p_{ox}}{1+k_2 p_{ox}}\right)X_A + k_B p_{ox}(1-X_A) \qquad \left(\frac{g}{cm^2.s}\right) \quad (22)$$

where: $X_A = \left(1+\frac{k_T}{k_B p_{ox}}\right)^{-1}$,

$k_A = 20\exp(-30000/RT)$,

$k_T = 1.51\times10^5\exp(-97000/RT)$,

$k_B = 4.46\times10^{-3}\exp(-15200/RT)$,

$k_2 = 21.3\times10^5\exp(4100/RT)$.

Multiplying S_c with the total surface area available for oxidation per soot volume (derived from net soot mass, soot density and mean soot particle diameter) gives the total soot oxidation rate. In this study a mean density of soot particle 2000 kg/m^3 and a mean soot size of 25 nm [18] was used.

Tailpipe Fluid Dynamic Sub-Model When the momentum equation is applied to the control volume within the tailpipe (which extends to the ends of the tailpipe), the forces include the pressure acting on the area at either end of the tailpipe, and the force generated by wall friction along the tailpipe length, F_f, are the only forces acting in the axial direction:

$$\left(p_e - p_o\right)A_e + F_f = \frac{du}{dt}\int_{tpv}\rho\, dV + u\left[\frac{d}{dt}\int_{tpv}\rho\, dV + \oint_{cs}\rho\,\vec{v}.\hat{n}ds\right] \quad (23)$$

The term in brackets on the right side is zero from conservation of mass. The integral of density is approximated as the product of the tailpipe entrance density, ρ_e, and the tailpipe volume. The tailpipe velocity is normalized with a characteristic velocity v_c defined as the velocity in the tailpipe that would exist for steady, isothermal, non-

reacting flow corresponding to the inlet mass flow rate:

$$v_c = \frac{m_i}{\rho_o A_e} = \frac{m_i}{\rho_o V}\frac{V}{A_e} = \frac{L_{c2}}{\tau_f} \tag{24}$$

where A_e is the tailpipe cross-section area, and the second length scale L_{c2} is the ratio of combustion volume to A_e. The friction force in Equation 23 is developed from the wall shear stress in terms of a conventional friction coefficient f as defined in [21]. Hence Equation 23 becomes:

$$\frac{d\tilde{u}}{dt} = (\tilde{p}_e - 1)\left(\frac{RT_o\tau_f}{L_{tp}L_{c2}}\right)\frac{\tilde{T}_e}{\tilde{p}_e} - \frac{L_{c2}f}{2D_{tp}\tau_f}\frac{\tilde{u}^3}{|\tilde{u}|} \tag{25}$$

where $\tilde{u}$ is the tailpipe normalized velocity, $\tilde{p}_e, \tilde{T}_e$ are pressure and temperature at the tailpipe entrance normalized with ambient conditions, L_{tp} and D_{tp} are the tailpipe length and diameter, respectively. With the aid of the tailpipe velocity and using the relation $m_e=\rho_e u A_e$, for use in Equations 11 and 12:

$$\frac{Z_e}{\rho_o} = \tilde{u}\frac{\tilde{p}_e}{\tilde{T}_e}\frac{1}{\tau_f} \tag{26}$$

This completes the development of the model. The simulation of the pulse combustor is achieved by solving the system of differential Equations 11, 12, 19 and 25. The solution of the system gives temperature, pressure, and mass fractions of fuel and oxygen in the combustion chamber and velocity in the tailpipe.

Inlet Mass Flow The configuration of the pulse combustor is an open air intake. This peculiarity makes the mixing process that governs the operation of the pulse combustor even more complicated. Not only there is interaction between heat release and the acoustic wave, but there is also coupling between the inlet mass flow and the acoustic flows. The way that the reactants are admitted in the combustor can affect the ignition delay time and in turn, the phase shift between heat release and acoustic wave [14]. The model is extended to relate the inlet mass flow of air with the pressure and the friction force in the inlet tailpipe. Due to a pressure of 200 kPa injection of fuel which takes place continuously the oscillation in the fuel line is neglected. Measurements of the air inlet flow suggest that the air inlet mass flow should be modeled as a sinusoidal function [22]. In reality the pressure in the air inlet pipe fluctuates around the atmospheric value, while the fuel inlet is driven by a high pressure upstream. Thus, the inlet mass flow of the air is modeled with a sinusoidal unsteady one.

$$m_i^{air} = C_1 + C_2 \sin(2\pi\ f_r t + \omega) \tag{27}$$

where f_r is the frequency of the sinusoidal inlet air mass flow (Hz), ω is the phase of the sinusoidal inlet mass flow (degree), and the parameters of the sinusoidal inlets were chosen from the experimental data. The values of the parameters used for the inlet flows are:
C_1 = 0.0105 kg/s,
C_2 = (2/3) C_1,
f_r = 150 Hz
and ω =180°.

Modification of Sinusoidal Inlet Since the flow in the open inlet is coupled to the internal flow, frequencies and amplitudes of these flows are related. Hence, frequency changes in one of these flows should influence the frequency of the other. Considering experimental results, a modification to the inlet flow is introduced to account for this feedback effect, in that the frequency of the inlet flow is adjusted to the internal frequency of oscillation at each time step. In this simulation the frequency of the inlet flow is related with a feedback mechanism to the frequency of the pressure oscillations in the combustion chamber, that was found to vary from 60 up to 80 Hz (T_w = 1000 K, h = 120 W/m^{2}K, f = 0.03). The sensitivity of the model to parameters C_1 and C_2 is now not as strong as it was with the previous simple sinusoidal inlet. With this updated model the simulated

oscillations of combustion are more irregular (Figure 5).

2. SYSTEM SOLUTION

A FORTRAN program compiled on PC calculates the solutions of the system employing a fourth-order Runge-Kutta scheme. In the program, a time step decrement/increment is used in order to achieve the best compromise between speed and accuracy of calculation. A list of geometric parameters (correspond to the experimental combustor) and other parameters required to run the program is as follow:

Ambient density	1.29 kg/m^3
Combustion zone volume	0.00496 m^3
Surface area combustion chamber	0.17842 m^2
First characteristic length	0.0278 m
Specific heat	1090 J/(kg K)
Ambient temperature	293 K
Specific heat ratio	1.374
Gas constant	287J/(kg K)
Tailpipe diameter	0.05 m
Tailpipe length	850 m
Second characteristic length	2.531 m
Heat transfer coefficient	120 W/m^{2}K
Inlet air mass flow rate (average)	0.05875kg/s
Friction factor	0.03
Initial fuel mass fraction	~0.06
A kinetic constant	3.85×10^8 m^{3}mol^{-1}s^{-1}
Heat of reaction per unit fuel mass	~33×10^6 J/kg

3. RESULTS

Theoretical results are performed for experimental pulse combustor of Beale [22]. The pulse combustor is Holmholtz type with open air inlet, hence the inlet flow supply is unsteady. However the model with steady inlet mass flow is initially used for the pulse combustor. The operational load of pulse combustor can varied between 60 to 260 kW of heat input.

Figure 2 shows the predicted pressure and temperature in the pulse combustor for steady inlet mass flows of fuel and air. The fuel inlet mass fraction is 0.065 and the wall temperature is 1000 K. The figure shows temperature and pressure oscillations from initial conditions (start-up) with some instability to 500 ms (stable condition). The initial pressure and temperature rises are caused by the initial conditions and suddenly occurrence of the reaction. However, the choice of initial conditions doesn't affect the final solutions. This result would be expected on physical grounds since the dissipative nature of friction in the tailpipe should negate the history of start-up. For steady inlet mass flows of fuel and air the variables of pressure and temperature vary periodically during the cycle of operation, which is characterized by a frequency of oscillation.

Figure 3 focuses attention on the frequency of oscillation and the phase shift between pressure and temperature in the pulse combustor with steady inlet mass flow rates. It can be seen that the model predicts a phase shift constant through the cycles. The predicted amplitudes of oscillations in pulse combustor are 150 K for temperature and about 0.25 atm for pressure.

Figure 4 presents the predicted unburned fuel mass fraction in the pulse combustor for three different values of the combustor wall temperature: 400 K (high heat loss), 1000 K (~ combustor normal condition) and 1400 K (high isolation). At the coldest wall temperature of 400 K, the combustion (fuel consumption) oscillation simply dies out after about 50 ms, and the flame is extinguished (fuel mass fraction increases sharply). At the highest wall temperature, 1400 K, the oscillation also dies out, but is replaced by a steady flame. This occurs because at the high 1400 K wall temperature, the associated higher gas temperature serves to increase the peak reaction rate, so that fuel consumption accelerates. The faster reactions which result from higher gas temperatures do not allow a surplus of fuel, so that a limited variation in reaction rate occurs, and the oscillation eventually dies out. Finally, for intermediate wall temperature, 1000 K, combustion (fuel consumption) oscillations continue. This is similar to the results obtained by Richards et al. [13] for the premixed combustion.

In a pulse combustor with high driving pressure upstream of the inlet pipes, the inlet flows are nearly steady when the inlet orifice is sized so to ensure choked flow. However, the experimental

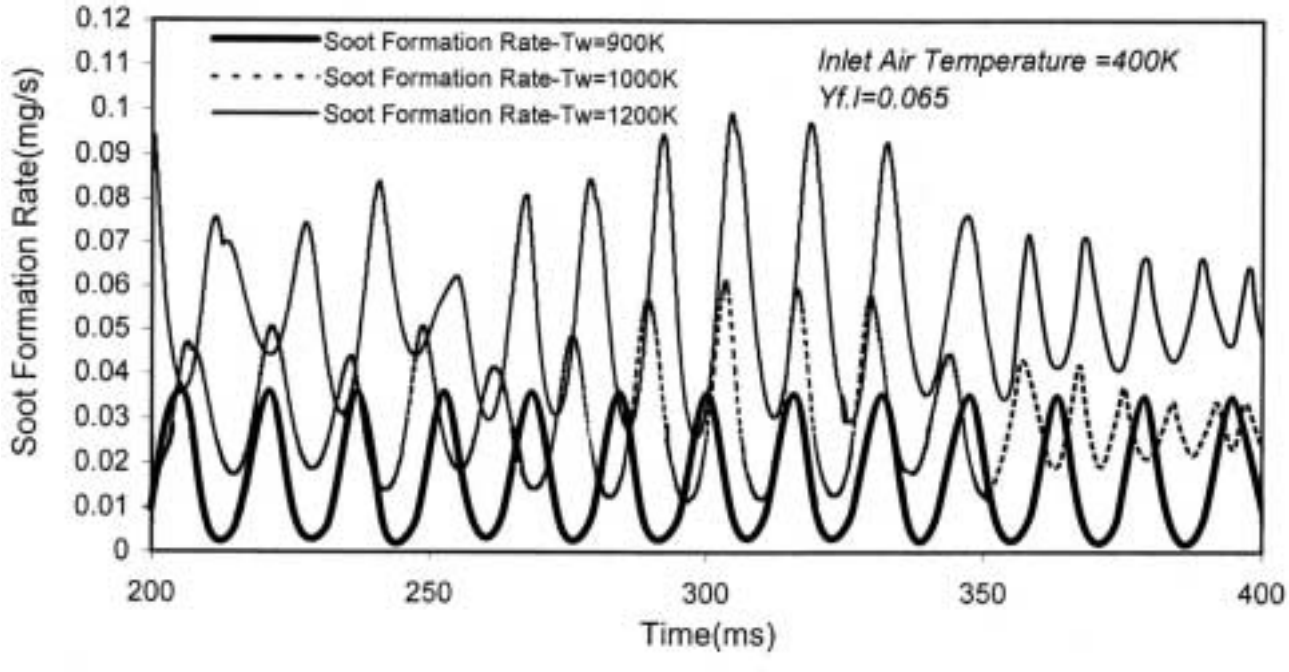

Figure 7. Effect of wall temperature on soot formation rate oscillationd.

pulse combustor of Beale [22] is with open air inlet, hence the inlet flow supply is unsteady. Using the sinusoidal inlet air mass flow (expression 27) for Beale's pulse combustor the instabilities of combustion oscillations were predicted. Figure 5 displays the calculated pressure oscillations of three inlet air configurations (steady inlet flow, sinusoidal inlet flow and modified sinusoidal inlet flow), and the comparison between the calculated and experimental measurements from 300 ms to1000 ms. It can be seen that with sinusoidal air inlet flow the simulated oscillations of pressure are irregular. Introduction of sinusoidally varying flow of air induces modulations of type observed in the experiments [22]. The comparison of the predicted oscillations of the modified sinusoidal inlet flow (coupling the frequency of the periodic flow of air with pressure oscillations within the combustor) with experimental results shows good agreement.

Figure 6 shows the comparison between the calculated fundamental frequencies of the combustion chamber pressure oscillation using modified inlet airflow with experimental measurements for different tailpipe lengths. It is appears that the theoretical predictions are in good agreement with the experimental data, particularly for longer tailpipe lengths. Both calculated and measured results show that the fundamental frequency increases with fuel input rate. The frequency of the shortest tailpipe, 737 mm, demonstrates the greatest sensitivity to fuel input rate changes. The 940 mm and 1930 mm tailpipe geometries exhibit relatively lower increase in the fundamental operating frequency for changing fuel input rates.

Figure 7 displays the calculated soot formation rate oscillations in the pulse combustor for three different combustor wall temperatures: 900 K, 1000 K and 1200 K, using the modified inlet air flow. The figure shows significant influence of wall temperature on both soot formation rate and soot oscillation amplitude. It is seen that an increase in wall temperature increases the soot

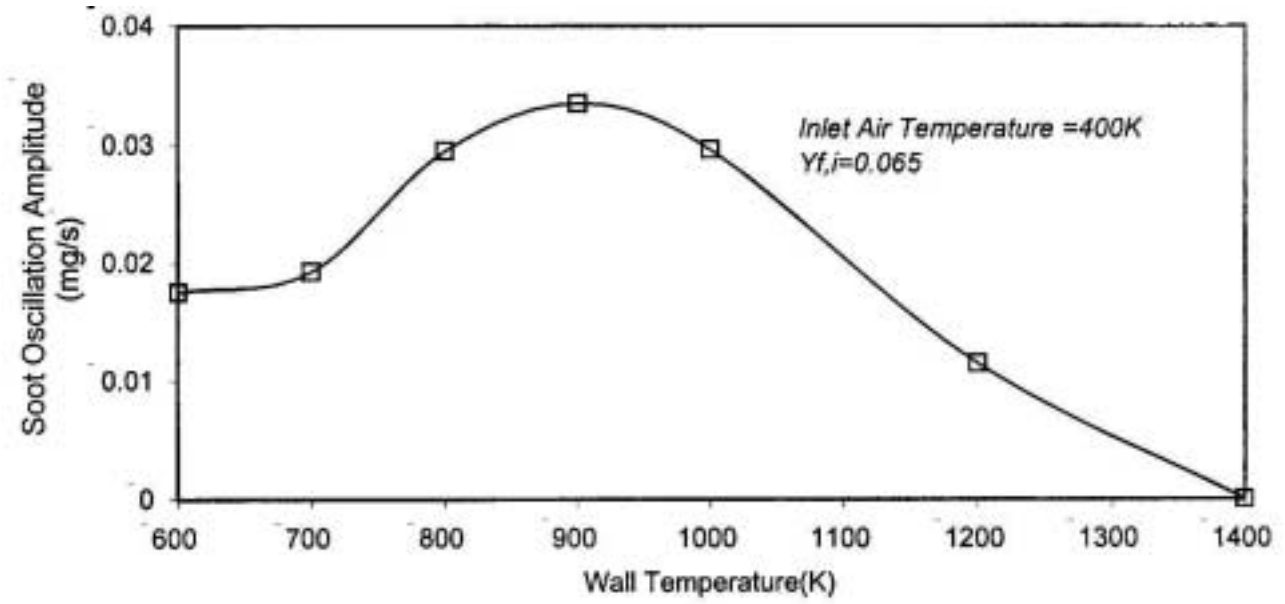

Figure 8. Effect of wall temperature on soot oscillation amplitude.

formation rate in the combustion chamber. It can be seen that at higher wall temperatures, 1000 K and 1200 K, the soot formation rate oscillations are not uniform and eventually die out (replaced by a steady condition). At combustor wall temperatures, 1000 K and 1200 K, the number of soot formation rate oscillations (before eventually dying out) was 22 and 55 respectively.

Figure 8 is a plot of the average peak-to-peak soot amplitude (before the oscillations eventually die out) as a function of the wall temperature (the summation of oscillation amplitudes has been divided by the number of oscillations). The figure shows that as the wall temperature increases the soot oscillation amplitude increases to a maximum and then reduces. The maximum soot oscillation amplitude is reached at wall temperature of 900 K. The reduction of soot oscillation amplitude at temperatures higher than 900 K is due to dying out of combustion oscillations and replacing by a steady flame (see Figure 4).

Predicted results of soot formation combustor output with different boundary conditions (inlet air temperature and combustor wall temperature) are shown in Figure 9. It can be seen that the maximum soot formation rate is reached at maximum inlet air temperature with highest wall temperature. This occurs because the processes of soot nucleation and surface growth are strongly temperature dependent [23], and clearly, the effect of higher wall temperature serves to increase the internal temperature of the combustor. For presented configuration it is seen that the predicted peak soot formation rate is about 0.05 mg/s and occurs at inlet air temperature = 400 K and wall temperature 1350 K. At the coldest inlet air temperature, 300 K, the production of soot is negligible, regardless of the combustor temperature is increased by wall temperature.

4. CONCLUSIONS

A homogeneous zero-dimensional model for simulation of pulse combustion aerovalved systems is developed and appraised against experiments so as to incorporate a sinusoidal air inlet mass flow coupled with pressure oscillations within the combustor and a soot formation-combustion model. The model is validated from

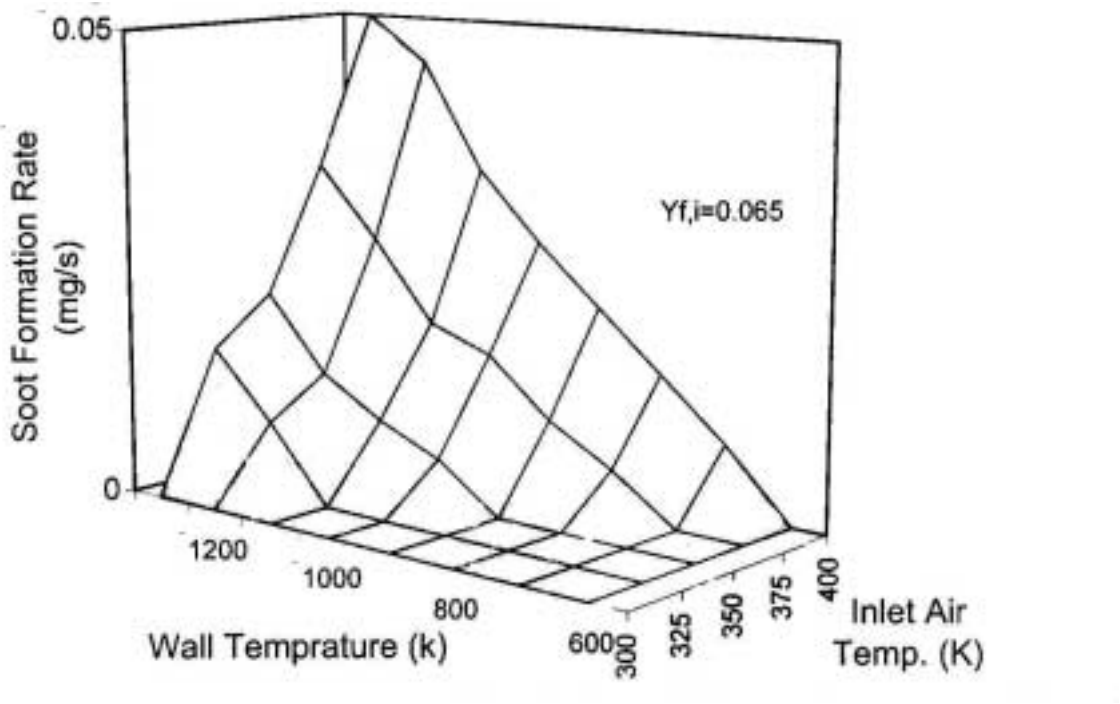

Figure 9. Effect of inlet air temperature and combustor wall temperature on soot format.

detailed experimental information on combustion oscillations available from an aerovalved Holmholts type firing propane. The model is able to reproduce the most peculiar characteristics of pulsating combustion such as amplitude modulations and running phase shift in the time-oscillations of the variables that characterize the pulse combustor process. As expected, the results show that soot emission from pulse combustors firing propane is very low particularly with ambient temperature of inlet air and normal combustor wall temperatures. At high wall and inlet air temperatures an increase in wall or inlet air temperature strongly increases the soot mass fraction.

5. REFERENCES

1. Putnam, A. A., Belles, F. E. and Kentfield, J. A. C., "Pulse Combustion", ***Progress in Energy and Combustion Science,*** Vol. 12, (1986), 43-79.
2. Keller, J. O., Bramlette, T. T., Barr, P. K. and Alvarez, J., "No_x and Coemissions from a Pulse Combustor Operating in Lean Premixed Mode", ***Combustion and Flame,*** Vol. 99, (1994), 460-466.
3. Penninger, A., Bereczky, A., Fernandes, E. C. and Horvath, A., "Some New Results in Development of Pulse Combustor", ***5th European Conference on Industrial Furnaces and Boilers,*** Porto-Portugal, (2000), 227-235.
4. Tajiri, K. and Menon, S., "LES of Combustion Dynamics in a Pulse Combustor", ***39th AIAA Aerospace Sciences Meeting and Exhibit,*** (January 2001), 87-96.
5. Kezerle, J. A., "Future Applications of Pulsating Combustion", ***Workshop in Pulsating, Combustion and Its Application***, Lund, Sweden, (1993), 63-69.
6. Kretschmer, D., and Odgers, J., "Modeling of Gas Turbine Combustors-A Convenient Reaction Rate Equation", ***Journal of Engineering for Power,*** (July 1972), 173-180.
7. Gemmen, R. S., Keller, J. O., Arpaci, V. S., "Heat/Mass Transfer From a Cylinder in the Strongly Oscillating Flow of a Pulse Combustor Tailpipe", ***Combustion Science and Technology,*** Vol. 94, No. 1-6, (1993), 103-130.
8. Dec, J. E. and Keller, J. O., "Pulse Combustor Tail-Pipe Heat-Transfer Dependence on Frequency, Amplitude, and Mean Flow Rate", ***Combustion and Flame***, Vol. 77, (1989), 359-374.

9. Lundgren, E. Marksten, U. and Moller, S. –I, "Enhancement of Heat Transfer in the Tail Pipe of Pulse Combustors", ***Symposium (International) on Combustion,*** Vol. 2, (1998), 3215-3220.
10. Inui, I., Okamoto, K., Nakamoto, M. and Hosaka, M., "Development of a Low Noise Pulse Combustor", ***Combust. Sci. Tech***.Vol. 52, (1987), 107-119.
11. Zinn, B. T., "Recent Applications and Research Issues (Invited Topical Review)", ***Twenty-Fourth Symposium (International) on Combustion,*** The Combustion Institute, (1992), 1297 –1305.
12. Moller, S. I. and Lindholm, A., "Theoretical and Experimental Investigation of the Operating Characteristics of a Holmholtz Type Pulse Combustor Due to Changes in the Inlet Geometry", ***Combustion Science and Technology***, Vol. 149, No. 1, (1999), 389-406.
13. Richards, G. A., Morris, G. J., Shaw D. W., Keely, S. A., Welter, M. J., "Thermal Pulse Combustion", ***Combustion Science and Technology,*** Vol. 94, (1993), 57-85.
14. Tsujimoto, Y. and Machii, N., "Numerical Analysis of a Pulse Combustion Burner", ***Twenty- First Symposium (International), on Combustion,*** The Combustion Institute, (1986), 1297-1305.
15. Morel, T., "Comprehensive Model of a Pulse Combustor", ***Combust. Sci. Tech.,*** Vol. 94, (1993), 379-409.
16. Bennelli, G., Cossalter, V. and Da Lio, M., "Advances in Numerical Simulation at ENEL", ***Combust. Sci. Tech.,*** Vol. 94, (1993.), 317-335
17. Glassman, I., "Combustion", 3th Edition, Academic Press, SanDiego, California, (1996).
18. Farmer, R., Edelman, R. and Wong, E., "Modeling Soot Emissions in Combustion Systems", Particulate Carbon, 299, Plenum Press, Canoga Park, California, (1981.)
19. Nagle, J. and Strickland-Constable, R. F., "Oxidation of Carbon Between 1000-2000 °C", ***Proc. Fifth Conference on Carbon,*** Pergamon, (1962), 154.
20. Stewart, C. D., Syed, K. J. and Moss, J. B., "Modeling Soot Formation in Non-Premixed Kerosine-Air Flames", ***Combust. Sci. and Tech.,*** Vol. **75,** (1991), 211-226.
21. Schlichting, H., "Boundary Layer Theory", McGraw-Hill, New York, (1979), 596-597.
22. Beale, A. J., "Aerovalved Pulse Combustion", PhD Thesis, University of Wales, Cardiff, (1999).
23. Brookes, S. J. and Moss, J. B., "Predictions of Soot And Thermal Radiation Properties in Confined Turbulent Jet Diffusion Flame", ***Combustion and Flame,*** Vol. 116, (1998), 486-503.